01 Aug 2014

Effect of the Center-Of-Mass Approximation on the Scaling of Electron-Capture Fully Differential Cross Sections

A. L. Harris

Don H. Madison
Missouri University of Science and Technology, madison@mst.edu

Recommended Citation

A. L. Harris and D. H. Madison, "Effect of the Center-Of-Mass Approximation on the Scaling of Electron-Capture Fully Differential Cross Sections," *Physical Review A - Atomic, Molecular, and Optical Physics*, vol. 90, no. 2, American Physical Society (APS), Aug 2014.
The definitive version is available at https://doi.org/10.1103/PhysRevA.90.022701

Effect of the center-of-mass approximation on the scaling of electron-capture fully differential cross sections

A. L. Harris[1,*] and D. H. Madison[2]

[1]*Physics Department, Illinois State University, Normal, Illinois 61790, USA*

[2]*Department of Physics, Missouri University of Science and Technology, Rolla, Missouri 65409, USA*

(Received 5 June 2014; published 4 August 2014)

We present results for p+He single electron capture and transfer with target excitation using the first Born approximation. The effect of approximating the center of mass of the helium atom and outgoing hydrogen atom at the respective nuclei is explored. Semianalytical results are compared for the calculations with and without the approximation, and it is shown that one must properly account for the center of mass of the atoms. It is also shown that this approximation is the result of the apparent v^4 scaling that was previously observed with the four-body transfer with target excitation model.

DOI: 10.1103/PhysRevA.90.022701 PACS number(s): 34.50.−s, 34.70.+e

I. INTRODUCTION

In recent years, an increasing amount of attention has been paid to charge transfer processes [1–7]. This is due in part to more detailed and accurate experimental data, which have prompted the development of new theoretical models aimed at better understanding the dynamics of charge transfer collisions. Two of these charge transfer processes are single electron capture (SC) and charge transfer with target excitation (TTE). For the case of proton-helium collisions, TTE corresponds to a proton colliding with a helium atom, capturing one of the target helium electrons, and leaving the collision as a neutral hydrogen atom in the ground state. The remaining electron in the He^+ ion is left in an excited state nl. The SC process is nearly identical to the TTE process, except that the residual He^+ ion is left in the ground state.

Within the literature, there has been an ongoing discussion over some observed differences between the four-body transfer with target excitation (4BTTE) model [8–10] and the plane-wave Born approximation (PWBA) model [2,11]. Results for these two models show discrepancies beyond what would be expected for calculations that are so similar. In particular, Chowdhury *et al.* [12] showed that the 4BTTE calculations were in worse agreement with experiment as the incident projectile energy increased. They found that the disagreement with experiment scaled as v^4, where v is the incident projectile velocity. When the 4BTTE model was divided by v^4, agreement with experiment was quite good. Houamer and Popov [11] suggested that this discrepancy was caused by a lack of numerical convergence in the 4BTTE calculation. However, this was shown not to be the case [12], despite the fact that Houamer and Popov continue to claim this [13]. As coauthors and developers of the 4BTTE model, it is obviously in our interest to resolve these discrepancies and to do this we have undertaken further investigation of our models.

In particular, we focus on the reference frame and coordinate system used in the 4BTTE model SC and TTE calculations, and the approximation that was made for this coordinate system. We show here that within the PWBA model, the fully differential cross sections (FDCSs) are highly sensitive to the coordinate system used, and that this is the cause of the v^4 scaling, not numerical errors as Houamer and Popov suggest. Atomic units (a.u.) are used throughout unless otherwise stated.

II. THEORY

From a theoretical and computational viewpoint, the SC and TTE processes are quite similar. In what follows, we choose to use p+He TTE as our example. When calculating a FDCS, it is important to specify the frame of reference for which the FDCS is being calculated. For example, one could choose to work within the lab frame, in which the initial target helium nucleus is at rest. This is the frame commonly used in the analysis of experiments. Alternatively, one could choose to work in the center-of-mass frame, where the center of mass of the entire system is at rest. The center-of-mass frame is more commonly used in theoretical calculations. The cross section for the 4BTTE model in the center-of-mass frame is

$$\frac{d\sigma}{d\Omega}^{C} = (2\pi)^4 \mu_{pa}\mu_{hi}\frac{k_f^C}{k_i^C}\left|T_{fi}^C\right|^2, \tag{1}$$

where μ_{pa} is the reduced mass of the projectile and target atom, μ_{hi} is the reduced mass of the hydrogen atom and residual He^+ ion, k_i^C is the magnitude of the incident projectile momentum in the center-of-mass frame, k_f^C is the magnitude of the scattered projectile momentum in the center-of-mass frame, and T_{fi}^C is the transition matrix in the center-of-mass frame. The center-of-mass FDCS can be converted into the lab frame FDCS by

$$\frac{d\sigma}{d\Omega}^{L} = \left[\frac{(1+2\gamma\cos\theta_C+\gamma^2)^{3/2}}{|1+\gamma\cos\theta_C|}\right]\frac{d\sigma}{d\Omega}^{C}, \tag{2}$$

where θ_C is the scattering angle of the projectile in the center-of-mass frame. The quantity γ is given by the ratio of the magnitude of the velocity of the center of mass of the entire collision system in the lab frame V and the magnitude of the scattered projectile velocity in the center-of-mass frame v_f^C, such that $\gamma = \frac{V}{v_f^C}$. The lab frame and center-of-mass frame scattering angles are related by

$$\tan\theta_L = \frac{\sin\theta_C}{\cos\theta_C+\gamma}. \tag{3}$$

*Corresponding author: alharri@ilstu.edu

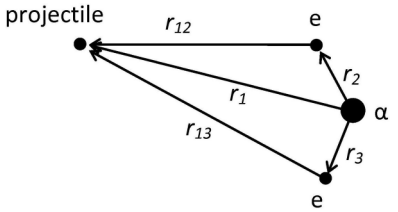

FIG. 1. Lab frame coordinates for a collision between a projectile and helium atom.

In order to perform a mostly analytical calculation in which numerical convergence is not a question, we will consider only the plane-wave Born approximation (PWBA) in which the projectile wave functions are all plane waves. The PWBA T matrix, in any reference frame, is given by

$$T_{fi} = \langle \Psi_f | V_i | \Psi_i \rangle, \tag{4}$$

where Ψ_f is the final-state wave function, Ψ_i is the initial-state wave function, and V_i is the perturbation potential given by the initial-state Coulomb interaction between the projectile and target helium atom,

$$V_i = \frac{2}{r_1} - \frac{1}{r_{12}} - \frac{1}{r_{13}}. \tag{5}$$

The distance from the projectile to the target nucleus is r_1, the distance from the projectile to one of the atomic electrons is r_{12}, and the distance from the projectile to the other atomic electron is r_{13} (see Fig. 1). It is important to point out that when a particular reference frame (such as the lab frame or the center-of-mass frame) is chosen for the calculation of the T matrix, the initial- and final-state wave functions will vary based on the reference frame.

Once a reference frame is chosen, one also has a choice of coordinate system to use in the calculation of the T matrix. In the lab frame, in which the target nucleus is at rest, the coordinates shown in Fig. 1 are a convenient choice of coordinates.

In the center-of-mass frame, in which the center of mass of the entire collision system is at rest, the Jacobi coordinates shown in Figs. 2 and 3 are a convenient choice of coordinates.

In the initial-state Jacobi coordinates, the vector $\vec{r}$ points from the target helium nucleus to the uncaptured electron, $\vec{s}$ points from the center of mass of the alpha-uncaptured electron system to the captured electron, and $\vec{R}_i$ points from the center of mass of the entire helium atom to the projectile. For the final-state Jacobi coordinates, $\vec{r}$ is unchanged, $\vec{y}$ points from the projectile to the captured electron, and $\vec{R}_f$ points from the center of mass of the He^+ ion to the center of mass of the outgoing hydrogen atom.

FIG. 2. Initial-state Jacobi coordinates.

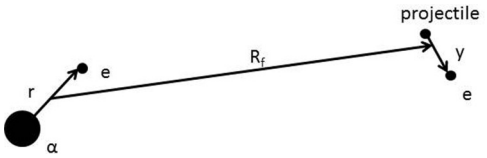

FIG. 3. Final-state Jacobi coordinates.

Then, the T matrix of Eq. (4) can be written as

$$T_{fi}^C = \int d\vec{R}_i d\vec{r} d\vec{s} \Psi_f^{C^*}(\vec{R}_i,\vec{r},\vec{s}) V_i(\vec{R}_i,\vec{r},\vec{s}) \Psi_i^C(\vec{R}_i,\vec{r},\vec{s}). \tag{6}$$

We note that the initial-state wave function is a simple expression in terms of $\vec{R}_i,\vec{r},\vec{s}$,

$$\Psi_i^C = \chi_{\vec{k}_i^C}(\vec{R}_i)\Phi_i^C(\vec{r},\vec{s}). \tag{7}$$

where $\Phi_i^C(\vec{r},\vec{s})$ is the helium atom wave function, and $\chi_{\vec{k}_i^C}(\vec{R}_i)$ is the incident projectile wave function. However, Ψ_f^C and V_i are not simple expressions using these coordinates. Fortunately, one can easily write $\vec{R}_i,\vec{r},\vec{s}$ in terms of $\vec{r}_1,\vec{r}_2,\vec{r}_3$ so that V_i can be expressed as in Eq. (5). Also, $\vec{R}_i,\vec{r},\vec{s}$ can be written in terms of $\vec{R}_f,\vec{r},\vec{y}$ so that Ψ_f^C can be written as

$$\Psi_f^C = \chi_{\vec{k}_f^C}(\vec{R}_f)\varphi_{He^+}^C(\vec{r})\varphi_H^C(\vec{y}), \tag{8}$$

where $\varphi_H^C(\vec{y})$ is the captured electron wave function, $\varphi_{He^+}^C(\vec{r})$ is the He^+ ion wave function, and $\chi_{\vec{k}_f^C}(\vec{R}_f)$ is the scattered projectile wave function. The initial and final projectile momenta in the center-of-mass frame are $\vec{k}_i^C$ and $\vec{k}_f^C$, respectively. Then, Eq. (6) becomes

$$T_{fi}^C = \int d\vec{R}_i d\vec{r} d\vec{s} \Psi_f^{C^*}(\vec{R}_f,\vec{r},\vec{y}) V_i(\vec{r}_1,\vec{r}_2,\vec{r}_3) \Psi_i^C(\vec{R}_i,\vec{r},\vec{s}) \tag{9}$$

where $\vec{r}_1,\vec{r}_2,\vec{r}_3$ and $\vec{R}_f,\vec{r},\vec{y}$ are written in terms of $\vec{R}_i,\vec{r},\vec{s}$.

Now, for the purposes of the analytical calculation, we perform a change of variables to $\vec{r}_1,\vec{r}_2,\vec{r}_3$ using

$$\begin{aligned} \vec{R}_i &= \vec{r}_1 - \frac{m_e}{m_{\text{nuc}} + 2m_e}(\vec{r}_2 + \vec{r}_3), \\ \vec{r} &= \vec{r}_3, \\ \vec{s} &= \vec{r}_2 - \frac{m_e}{m_{\text{nuc}} + m_e}\vec{r}_3, \end{aligned} \tag{10}$$

and

$$\begin{aligned} \vec{R}_f &= \frac{m_p\vec{r}_1 + m_e\vec{r}_2}{m_p + m_e} - \frac{m_e}{m_{\text{nuc}} + m_e}\vec{r}_3, \\ \vec{r} &= \vec{r}_3, \\ \vec{y} &= \vec{r}_2 - \vec{r}_1, \end{aligned} \tag{11}$$

where m_e is the mass of the electron, m_{nuc} is the mass of the helium nucleus, and m_p is the mass of the proton.

The Jacobian determinant for the coordinate transformation is unity, and the center-of-mass T matrix becomes

$$T_{fi}^C = \int d\vec{r}_1 d\vec{r}_2 d\vec{r}_3 \Psi_f^{C^*}(\vec{R}_f,\vec{r},\vec{y}) V_i(\vec{r}_1,\vec{r}_2,\vec{r}_3) \Psi_i^C(\vec{R}_i,\vec{r},\vec{s}). \tag{12}$$

In our previous work [8–10], we chose to work in the center-of-mass frame with the Jacobi coordinates. However, we made the approximation that the center of mass of the helium atom and He^+ ion are both located at the target nucleus, and the center of mass of the hydrogen atom is located at the proton. Then the Jacobi coordinates become

$$\vec{R}_i \approx \vec{r}_1, \quad \vec{r} = \vec{r}_3, \quad \vec{s} \approx \vec{r}_2, \tag{13}$$

and

$$\vec{R}_f \approx \vec{r}_1, \quad \vec{r} = \vec{r}_3, \quad \vec{y} = \vec{r}_2 - \vec{r}_1. \tag{14}$$

An alternative way of stating this approximation is that $m_e \ll m_p$ and $m_e \ll m_{\rm nuc}$.

To explore the validity of this approximation without introducing the issue of numerical convergence, we need to compare analytical calculations for SC and TTE using both the Jacobi coordinates $\vec{R}_f,\vec{r},\vec{y}$ and $\vec{R}_i,\vec{r},\vec{s}$ and the approximation of the Jacobi coordinates as $\vec{r}_1,\vec{r}_2,\vec{r}_3$. In the remainder of this paper, when the $\vec{r}_1,\vec{r}_2,\vec{r}_3$ vectors are used to approximate $\vec{R}_f,\vec{r},\vec{y}$ and $\vec{R}_i,\vec{r},\vec{s}$, we will refer to this as the "lab approximation" because $\vec{r}_1,\vec{r}_2,\vec{r}_3$ are the coordinates that one would use if calculating the T matrix in the lab frame. When the $\vec{R}_f,\vec{r},\vec{y}$ and $\vec{R}_i,\vec{r},\vec{s}$ vectors are used, we will call this the "Jacobi calculation."

A. Jacobi calculation

We begin with the Jacobi calculation, where the FDCS is calculated in the center of mass frame using Jacobi coordinates. We point out that the final-state outgoing hydrogen momentum is slightly different for SC than for TTE due to the slightly larger projectile energy loss that is required to excite the He^+ ion. While this difference is generally negligible, we do include it in our calculations. The Jacobi calculation T matrix is written as

$$T_{fi}^J = \int d\vec{r}_1 d\vec{r}_2 d\vec{r}_3 \chi^*_{\vec{k}_f^C}(\vec{R}_f)\varphi^{C^*}_{\rm He^+}(\vec{r})\varphi^{C^*}_{\rm H}(\vec{y})V_i(\vec{r}_1,\vec{r}_2,\vec{r}_3)\chi_{\vec{k}_i^C}(\vec{R}_i)\Phi_i^C(\vec{r},\vec{s}). \tag{15}$$

Plugging in V_i, Eq. (15) can be written as a sum of three terms,

$$T_{fi}^J = T_1^J + T_{12}^J + T_{13}^J, \tag{16}$$

where

$$T_1^J = \int d\vec{r}_1 d\vec{r}_2 d\vec{r}_3 \chi^*_{\vec{k}_f^C}(\vec{R}_f)\varphi^{C^*}_{\rm He^+}(\vec{r})\varphi^{C^*}_{\rm H}(\vec{y})\left(\frac{2}{r_1}\right)\chi_{\vec{k}_i^C}(\vec{R}_i)\Phi_i^C(\vec{r},\vec{s}), \tag{17}$$

$$T_{12}^J = \int d\vec{r}_1 d\vec{r}_2 d\vec{r}_3 \chi^*_{\vec{k}_f^C}(\vec{R}_f)\varphi^{C^*}_{\rm He^+}(\vec{r})\varphi^{C^*}_{\rm H}(\vec{y})\left(\frac{-1}{r_{12}}\right)\chi_{\vec{k}_i^C}(\vec{R}_i)\Phi_i^C(\vec{r},\vec{s}), \tag{18}$$

$$T_{13}^J = \int d\vec{r}_1 d\vec{r}_2 d\vec{r}_3 \chi^*_{\vec{k}_f^C}(\vec{R}_f)\varphi^{C^*}_{\rm He^+}(\vec{r})\varphi^{C^*}_{\rm H}(\vec{y})\left(\frac{-1}{r_{13}}\right)\chi_{\vec{k}_i^C}(\vec{R}_i)\Phi_i^C(\vec{r},\vec{s}). \tag{19}$$

In the plane-wave Born approximation, the wave functions for the incident and scattered projectile are given by plane waves,

$$\chi_{\vec{k}_i^C}(\vec{R}_i) = \frac{e^{i\vec{k}_i^C\cdot\vec{R}_i}}{(2\pi)^{3/2}}, \tag{20}$$

$$\chi_{\vec{k}_f^C}(\vec{R}_f) = \frac{e^{i\vec{k}_f^C\cdot\vec{R}_f}}{(2\pi)^{3/2}}. \tag{21}$$

To allow for a mostly analytical solution, we use a variational product wave function for the helium ground state, which is given by

$$\begin{aligned}\Phi_i^C(\vec{r},\vec{s}) &\approx \Phi_i(\vec{r}_2,\vec{r}_3),\\ &= \frac{\alpha^3}{\pi}e^{-\alpha(r_2+r_3)}\end{aligned} \tag{22}$$

where $\alpha = 1.6875$. This approximation is reasonable since by definition $|\vec{r}| = |\vec{r}_3|$. Also, the approximation of $|\vec{s}| \approx |\vec{r}_2|$ can be seen from $|\vec{s}| \approx \sqrt{s^2 + 2\frac{m_e}{m_{\rm nuc}+m_e}\vec{s}\cdot\vec{r}}$, where we have neglected the second-order term. Because the ground-state helium atom wave function is highly localized, the radial distance of both electrons is similar in magnitude, making the second term in the square root negligible compared to the first term.

In this paper, we will examine both SC and TTE with the helium ion left in the $2s$ state. The $2s$ state was chosen because the magnitude of the FDCS drops off quickly with increasing n, and s states are the dominant contribution to the TTE FDCS. We point out that by using a product helium ground-state wave function, the cross section for TTE to any of the $2p$ states is zero due to orthogonality between the initial and final bound helium and He^+ wave functions. The final-state bound wave functions are all hydrogenic wave functions given by

$$\varphi^{1s}_{\rm He^+}(\vec{r}) = \frac{2^{3/2}e^{-2r}}{\sqrt{\pi}}, \tag{23}$$

$$\varphi^{2s}_{\rm He^+}(\vec{r}) = \frac{(1-r)e^{-r}}{\sqrt{\pi}}, \tag{24}$$

$$\varphi_{\rm H}(\vec{y}) = \frac{e^{-y}}{\sqrt{\pi}}. \tag{25}$$

Plugging in the individual wave function expressions for SC yields

$$T_1^{J\text{-SC}} = \frac{128\sqrt{2}\alpha^4(2+\alpha)}{\pi^4[(2+\alpha)^2+n^2]^2}\int d\vec{t}\,\frac{1}{(1+t^2)^2(\vec{s}_0-\vec{t})^2[\alpha^2+(\vec{t}-\vec{p})^2]^2}, \tag{26}$$

$$T_{12}^{J\text{-SC}} = \frac{-64\alpha^4(2+\alpha)\sqrt{2}}{\pi^2}\frac{1}{[(2+\alpha)^2+n^2]^2[\alpha^2+(\vec{s}_0-\vec{p})^2]^2\left(s_0^2+1\right)}, \tag{27}$$

$$T_{13}^{J\text{-SC}} = \frac{-64\sqrt{2}\alpha^4(2+\alpha)}{\pi^4}\int d\vec{t}\,\frac{1}{(1+t^2)^2[(2+\alpha)^2+(\vec{n}-\vec{s}_0+\vec{t})^2]^2(\vec{s}_0-\vec{t})^2[\alpha^2+(\vec{p}-\vec{t})^2]^2}, \tag{28}$$

where the Fourier transform of the $1s$ hydrogen wave function has been used,

$$\varphi_{\rm H}(\vec{y}) = \frac{1}{(2\pi)^3}\int d\vec{t}e^{-i\vec{t}\cdot\vec{y}}\varphi_{\rm H}^F(\vec{t}), \tag{29}$$

with

$$\varphi_{\rm H}^F(\vec{t}) = \int d\vec{r}_{12}e^{i\vec{t}\cdot\vec{r}_{12}}\varphi_{\rm H}(\vec{r}_{12}) = \frac{8\sqrt{\pi}}{(1+t^2)^2}. \tag{30}$$

Also,

$$\vec{s}_0 = \vec{k}_i^c - \frac{m_p}{m_p+m_e}\vec{k}_f^c, \tag{31}$$

$$\vec{p} = \frac{m_e}{m_{\rm nuc}+2m_e}\vec{k}_i^c + \frac{m_e}{m_p+m_e}\vec{k}_f^c, \tag{32}$$

$$\vec{n} = \frac{m_e}{m_{\rm nuc}+2m_e}\vec{k}_i^c - \frac{m_e}{m_{\rm nuc}+m_e}\vec{k}_f^c. \tag{33}$$

The $T_1^{J\text{-SC}}$ integral can be further reduced to a one-dimensional integral by following the procedure outlined in [14], and the three-dimensional $T_{13}^{J\text{-SC}}$ integral is performed numerically using Gauss-Legendre quadrature.

For TTE to the $2s$ state, the corresponding expressions for the T matrix in the Jacobi calculation are

$$T_1^{J\text{-TTE}} = \frac{[(1+\alpha)^2(\alpha-2)+n^2(2+\alpha)][(2+\alpha)^2+n^2]^2}{2^{3/2}[(1+\alpha)^2+n^2]^3(2+\alpha)}T_1^{J\text{-SC}}, \tag{34}$$

$$T_{12}^{J\text{-TTE}} = \frac{[(1+\alpha)^2(\alpha-2)+n^2(2+\alpha)][(2+\alpha)^2+n^2]^2}{2^{3/2}[(1+\alpha)^2+n^2]^3(2+\alpha)}T_{12}^{J\text{-SC}}, \tag{35}$$

$$T_{13}^{J\text{-TTE}} = \frac{-32\alpha^4}{\pi^4}\int d\vec{t}\,\frac{[(\alpha-2)(1+\alpha)^2+(2+\alpha)(\vec{s}_0-\vec{t}-\vec{n})^2]}{(1+t^2)^2[(1+\alpha)^2+(\vec{s}_0-\vec{t}-\vec{p})^2]^2(\vec{s}_0-\vec{t})^2[\alpha^2+(\vec{p}-\vec{t})^2]^2}. \tag{36}$$

Again, the three-dimensional $T_{13}^{J\text{-TTE}}$ integral is performed numerically using Gauss-Legendre quadrature.

B. Lab approximation

Following a similar procedure to the Jacobi calculation, the lab approximation T matrix is written as a sum of three terms:

$$T_{fi}^{\rm LA} = T_1^{\rm LA} + T_{12}^{\rm LA} + T_{13}^{\rm LA}, \tag{37}$$

where

$$T_1^{\rm LA} = \int d\vec{r}_1 d\vec{r}_2 d\vec{r}_3 \chi_{\vec{k}_f^C}^*(\vec{r}_1)\varphi_{\rm He^+}^{C^*}(\vec{r}_3)\varphi_{\rm H}^{C^*}(\vec{r}_{12})\left(\frac{2}{r_1}\right)\chi_{\vec{k}_i^C}(\vec{r}_1)\Phi_i^C(\vec{r}_2,\vec{r}_3), \tag{38}$$

$$T_{12}^{\rm LA} = \int d\vec{r}_1 d\vec{r}_2 d\vec{r}_3 \chi_{\vec{k}_f^C}^*(\vec{r}_1)\varphi_{\rm He^+}^{C^*}(\vec{r}_3)\varphi_{\rm H}^{C^*}(\vec{r}_{12})\left(\frac{-1}{r_{12}}\right)\chi_{\vec{k}_i^C}(\vec{r}_1)\Phi_i^C(\vec{r}_2,\vec{r}_3), \tag{39}$$

$$T_{13}^{\rm LA} = \int d\vec{r}_1 d\vec{r}_2 d\vec{r}_3 \chi_{\vec{k}_f^C}^*(\vec{r}_1)\varphi_{\rm He^+}^{C^*}(\vec{r}_3)\varphi_{\rm H}^{C^*}(\vec{r}_{12})\left(\frac{-1}{r_{13}}\right)\chi_{\vec{k}_i^C}(\vec{r}_1)\Phi_i^C(\vec{r}_2,\vec{r}_3). \tag{40}$$

The incident and scattered projectile wave functions are given by plane waves,

$$\chi_{\vec{k}_i^C}(\vec{r}_1) = \frac{e^{i\vec{k}_i^C\cdot\vec{r}_1}}{(2\pi)^{3/2}}, \tag{41}$$

$$\chi_{\vec{k}_f^C}(\vec{r}_1) = \frac{e^{i\vec{k}_f^C\cdot\vec{r}_1}}{(2\pi)^{3/2}}, \tag{42}$$

and the variational product helium ground-state wave function is again

$$\Phi_i^C(\vec{r}_2,\vec{r}_3) = \frac{\alpha^3}{\pi}e^{-\alpha(r_2+r_3)}. \tag{43}$$

Using the approximation that $m_e \ll m_{\rm nuc}$ and $m_e \ll m_p$, Eqs. (31)–(33) become

$$\vec{s}_0 \approx \vec{k}_i^c - \vec{k}_f^c = \vec{q}, \tag{44}$$

$$\vec{p} \approx 0, \tag{45}$$

$$\vec{n} \approx 0. \tag{46}$$

Then, the T matrix terms of Eqs. (26)–(28) become

$$T_1^{\text{LA-SC}} = \frac{128\alpha^4\sqrt{2}}{\pi^4(2+\alpha)^3}\int d\vec{t}\,\frac{1}{(\alpha^2+t^2)^2(\vec{q}-\vec{t})^2(1+t^2)^2}, \tag{47}$$

$$T_{12}^{\text{LA-SC}} = \frac{-64\alpha^4\sqrt{2}}{\pi^2(\alpha^2+q^2)^2(2+\alpha)^3(q^2+1)}, \tag{48}$$

$$T_{13}^{\text{LA-SC}} = \frac{-64\alpha^4\sqrt{2}(2+\alpha)}{\pi^4}\int d\vec{t}\,\frac{1}{(\alpha^2+t^2)^2(\vec{q}-\vec{t})^2(1+t^2)^2[(2+\alpha)^2+(\vec{q}-\vec{t})^2]^2}, \tag{49}$$

and Eqs. (34)–(36) become

$$T_1^{\text{LA-TTE}} = \frac{(\alpha-2)(2+\alpha)^3}{(1+\alpha)^4 2^{3/2}}T_1^{\text{LA-SC}}, \tag{50}$$

$$T_{12}^{\text{LA-TTE}} = \frac{-32\alpha^4(\alpha-2)}{\pi^2(\alpha^2+q^2)^2(1+\alpha)^4(q^2+1)}, \tag{51}$$

$$T_{13}^{\text{LA-TTE}} = \frac{-32\alpha^4}{\pi^4}\int d\vec{t}\,\frac{[(2+\alpha)(\vec{q}-\vec{t})^2+(1+\alpha)^2(\alpha-2)]}{(\alpha^2+t^2)^2(\vec{q}-\vec{t})^2(1+t^2)^2[(1+\alpha)^2+(\vec{q}-\vec{t}^2)]^2}. \tag{52}$$

The $T_{13}^{\text{LA-TTE}}$ integral can again be reduced to a one-dimensional integral through contour integration, and the one-dimensional integrals that remain are calculated numerically using Gauss-Legendre quadrature.

We would like to note that Houamer and Popov [2,12,15] make a similar approximation to the lab approximation described here. Specifically, they use $m_e \ll m_{\rm nuc}$, which is the same approximation we use to get from Eq. (10) to Eq. (13), and yields an initial-state projectile wave function of

$$\chi_{\vec{k}_i^C}(\vec{R}_i) \approx \chi_{\vec{k}_i^C}(\vec{r}_1). \tag{53}$$

This the same as our lab approximation of Eq. (41). However, $m_e \ll m_{\rm nuc}$ does not by itself lead from our Eq. (11) to Eq. (14). Instead, using it leads to Eq. (11) becoming

$$\begin{aligned}\vec{R}_f &\approx \frac{m_p\vec{r}_1 + m_e\vec{r}_2}{m_p+m_e},\\ \vec{r} &= \vec{r}_3,\\ \vec{y} &= \vec{r}_2 - \vec{r}_1,\end{aligned} \tag{54}$$

and the final-state projectile plane wave of

$$\chi_{\vec{k}_f^C}(\vec{R}_f) \approx \exp\left[i\frac{m_p}{m_p+m_e}\vec{k}_f^C\cdot\vec{r}_1\right]\exp\left[i\frac{m_e}{m_p+m_e}\vec{k}_f^C\cdot\vec{r}_2\right]. \tag{55}$$

This is different than our lab approximation of Eq. (42), and it is at this point that Houamer and Popov use $m_e \ll m_p$ to get

$$\chi_{\vec{k}_f^C}(\vec{R}_f) \approx \exp\left[i\vec{k}_f^C\cdot\vec{r}_1\right]\exp\left[i\vec{k}_f^C\cdot\vec{r}_2/m_p\right]. \tag{56}$$

Clearly, it is this second term in the above equation that is crucially missing in our lab approximation.

III. RESULTS

A. Single electron capture

Figure 4 shows FDCS results comparing the lab approximation to the Jacobi calculation for p+He SC at incident proton energies between 25 and 500 keV. Because the previous work by Chowdhury *et al.* [10] found that the 4BTTE model overestimated experiment by approximately a factor of v^4, where v is the incident proton velocity, we also show results of

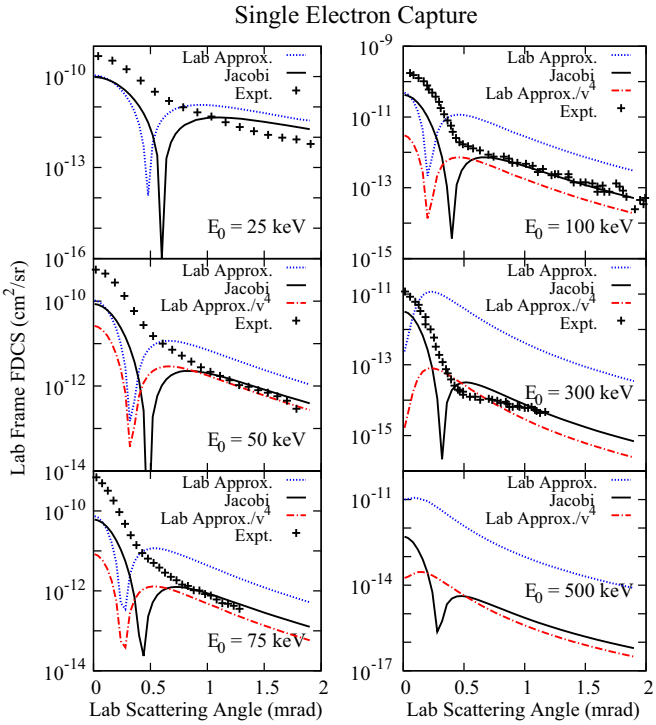

FIG. 4. (Color online) Results for p+He single capture for the Jacobi calculation (solid line), the lab approximation (dotted line), and the lab approximation divided by the incident proton velocity to the fourth power (dash-dotted line). Absolute experiment is from [1] (25–75 keV) and [16] (100 and 300 keV).

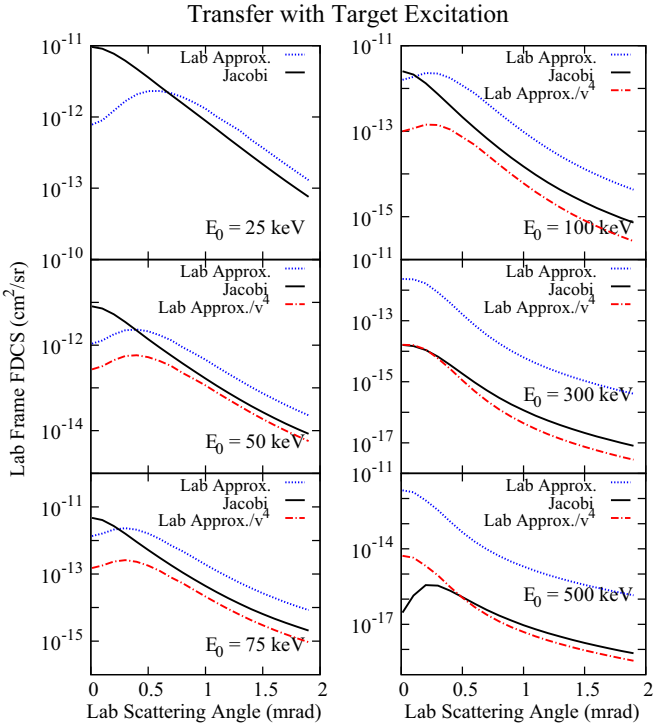

FIG. 5. (Color online) Results for p+He transfer with target excitation for the Jacobi calculation (solid line), the lab approximation (dotted line), and the lab approximation divided by the incident proton velocity to the fourth power (dash-dotted line).

the lab approximation divided by v^4. The PWBA theoretical results are compared to the absolute experiment of Hasan [1] and Schöffler [16].

It can be seen from Fig. 4 that at the lowest energy, the lab approximation and Jacobi calculations are generally similar in magnitude and shape. There is a slight shift in the location of the deep minimum in the lab approximation compared to the Jacobi calculation, with the lab approximation predicting the minimum at a smaller scattering angle than the Jacobi calculation. As the incident proton energy increases, the two calculations remain similar in shape, but diverge in magnitude. We note that the PWBA becomes a more valid approximation as the incident energy increases. For an incident proton energy of 25 keV, the perturbation $\frac{Z_p}{v_p} = 1$ where Z_p is the projectile charge and v_p is the projectile velocity. Typically, one considers the PWBA valid when $\frac{Z_p}{v_p} < 1$, which indicates that 25 keV is on the low end of validity for the PWBA.

The results of the lab approximation divided by v^4 indicate that the cause of the previously observed scaling factor is clearly the result of approximating the Jacobi coordinates as the lab coordinates. Thus, it is clear that one must be extremely careful in the approximations that are made, and that the lab approximation we used is not a valid approximation for SC.

B. Transfer with target excitation

In Fig. 5 we compare the lab approximation and Jacobi calculation for TTE to the $2s$ state. Again it can be seen that for low energies, the lab approximation calculations are similar in magnitude to the Jacobi calculations. However, the lab approximation calculation exhibits a peak structure that is not seen in the Jacobi calculation. At large scattering angles, the difference in magnitude scales approximately as v^4, just as in the SC case. This once again indicates that approximating the Jacobi coordinates as the lab coordinates is not a valid approximation, and is the cause of the apparent v^4 scaling that was previously observed. We note that experiment is not included in Fig. 5 because the analytical results in this paper are only for TTE to the $2s$ state, while experiment includes contributions from all excited states.

While it is clear that the lab approximation leads to the apparent v^4 scaling for both SC and TTE, we have not been able to find an intuitive physical explanation for this particular scaling. As far as we can tell, it is simply an artifact of an invalid approximation.

Upon completion of the PWBA analytical calculations for SC and TTE, we returned to our 4BTTE calculation and code to perform calculations that did not approximate the Jacobi coordinates as the lab coordinates. However, we were unable to achieve numerical convergence for the full numerical nine-dimensional integral when the Jacobi coordinates were used, but it was possible to obtain convergence when the Jacobi coordinates were approximated as the lab coordinates, as shown in [10]. It was this difficulty with convergence that prompted us to make the approximation of the Jacobi coordinates in the first place. However, the large discrepancies in magnitude did not appear until we turned our attention to higher projectile energies

[8–10]. We also performed a few calculations using our 4BTTE nine-dimensional code with the lab coordinates, the simple variational helium ground-state wave function of Eq. (22), and plane waves for the incident and scattered projectile. The results of the 4BTTE numerical calculations agreed with the semianalytical lab approximation calculations presented here, as they should.

IV. CONCLUSION

In conclusion, we have conducted a thorough investigation into the plane-wave Born approximation for single electron capture and transfer with target excitation in the center-of-mass frame using both Jacobi coordinates and an approximation of the Jacobi coordinates as the lab coordinates. It was found that for single electron capture and transfer with target excitation at low incident projectile energies, the Jacobi calculation and the lab approximation calculation were similar. However, for large incident projectile energies, the calculations diverge from each other. Some structural differences were also observed in the lab approximation compared to the Jacobi calculation.

We have also shown that the use of the lab approximation by Chowdhury *et al.* [10] is the cause of the four-body transfer with target excitation model overestimating experiment by a factor of v^4, not numerical error. These results all indicate that when calculating single capture and transfer with target excitation fully differential cross sections in the center-of-mass frame, it is imperative to not approximate the Jacobi coordinates as the lab coordinates in spite of the fact that this might seem like a very reasonable approximation.

ACKNOWLEDGMENT

We would like to thank Y. Popov for many useful discussions.

[1] A. Hasan, B. Tooke, M. Zapukhlyak, T. Kirchner, and M. Schulz, Phys. Rev. A **74**, 032703 (2006).
[2] H.-K. Kim, M. S. Schöffler, S. Houamer, O. Chuluunbaatar, J. N. Titze, L. Ph. H. Schmidt, T. Jahnke, H. Schmidt-Böcking, A. Galstyan, Yu. V. Popov, and R. Dörner, Phys. Rev. A **85**, 022707 (2012).
[3] I. Mančev, N. Milojević, and D. Belkić, Phys. Rev. A **86**, 022704 (2012).
[4] M. S. Schöffler, J. N. Titze, L. Ph. H. Schmidt, T. Jahnke, O. Jagutzki, H. Schmidt-Böcking, and R. Dörner, Phys. Rev. A **80**, 042702 (2009).
[5] D. L. Guo, X. Ma, S. F. Zhang, X. L. Zhu, W. T. Feng, R. T. Zhang, B. Li, H. P. Liu, S. C. Yan, P. J. Zhang, and Q. Wang, Phys. Rev. A **86**, 052707 (2012).
[6] M. Purkait and R. Samanta, Phys. Scr. **84**, 065301 (2011).
[7] E. Ghanbari-Adivi, J. Phys. B: At. Mol. Opt. Phys. **44**, 165204 (2011).
[8] A. L. Harris, J. L. Peacher, D. H. Madison, and J. Colgan, Phys. Rev. A **80**, 062707 (2009).
[9] A. L. Harris, J. L. Peacher, and D. H. Madison, Phys. Rev. A **82**, 022714 (2010).
[10] U. Chowdhury, A. L. Harris, J. L. Peacher, and D. H. Madison, J. Phys. B: At. Mol. Opt. Phys. **45**, 035203 (2012).
[11] S. Houamer and Yu. V. Popov, J. Phys. B: At. Mol. Opt. Phys. **46**, 028001 (2013).
[12] U. Chowdhury, A. L. Harris, J. L. Peacher, and D. H. Madison, J. Phys. B: At. Mol. Opt. Phys. **46**, 028002 (2013).
[13] M. S. Schöffler, H.-K. Kim, O. Chuluunbaatar, S. Houamer, A. G. Galstyan, J. N. Titze, T. Jahnke, L. Ph. H. Schmidt, H. Schmidt-Böcking, R. Dörner, Yu. V. Popov, and A. A. Bulychev, Phys. Rev. A **89**, 032707 (2014).
[14] M. R. C. McDowell and J. P. Coleman, *Introduction to the Theory of Ion-Atom Collisions* (North-Holland Publishing Co., Amsterdam, 1970), Appendix 8.1.
[15] Y. Popov (personal communication).
[16] M. S. Schöffler, J. Titze, L. Ph. H. Schmidt, T. Jahnke, N. Neumann, O. Jagutzki, H. Schmidt-Böcking, R. Dörner, and I. Mančev, Phys. Rev. A **79**, 064701 (2009).